

Nonlinear Speed Control of Permanent Magnet Synchronous Motor with Salient Poles

K. Kyslan^{1*}, V. Šlapák¹, M. Pajkoš², F. Ďurovský¹

¹Department of Electrical Engineering and Mechatronics, Faculty of Electrical Engineering and Informatics, Technical University of Košice, Letná 9, 042 00, Košice, Slovak Republic

²Spinea Technologies s.r.o., Volgogradská 13, 080 05 Prešov, Slovak Republic

Received 25 November 2015; Accepted 28 December 2015

Abstract

This paper presents the speed control of permanent magnet synchronous motor with salient poles based on two-step linearization method. In the first step, the direct compensation of the nonlinearities in the equations of current is used. In the second step, the input-output linearization in the state space is used for the decoupling of flux and torque axis. Simulated results are compared to the field oriented vector control structure with PI controllers in order to show differences in the performance of both approaches.

Keywords: nonlinear control, permanent magnet synchronous machine, feedback linearization, transformation matrix, nonlinear canonical form

1. Introduction

Permanent magnet synchronous motors (PMSM) are widely used in a large number of applications demanding very high dynamic performance. Current research on the PMSM control is mainly focused on the sensorless control methods. These are either based on the motor fundamental equations, as the back EMF integration [1], extended Kalman filter [2], or sliding mode observer [3]. The common problem of these methods is that the performance of the position estimations is dependent on the back EMF voltage, which is small in a low speed region and thus the performance is degraded. Various techniques were presented to improve this performance, such as in [4] or [5].

Nevertheless, there are applications where the sensorless control is not required and still the best performance is achieved with the use of a sensor at the rotor shaft. Therefore, there is a constant need for research in the field of the control designs with the sensor. Authors, dealing with the nonlinear modelling and control of PMSM with the sensor, presented interesting techniques. In [6], sliding-mode control and extended sliding-mode disturbance observer was introduced in order to considerably improve the dynamic performance. Model reference adaptive control for the sensor application was presented in [7]. Current research on the sensor control involves the use of FPGA circuits [8], low resolution sensors for high performance [9], the application of predictive control methods [10] or the energy efficient control [11].

An assumption of round rotor (i.e. $L_d=L_q$, non-saliency) makes overall model of PMSM easier to control. Considering the impact of the saliency effect, additional nonlinearity will appear in the model and overall nonlinear

control design becomes more complicated in the term of decoupling demands. Modelling of various saliency effects was presented in [12]. A variety of approaches can be used for nonlinear control of PMSM, such as input-output linearization [13] or sliding-mode control [14]. In this paper, we present nonlinear control of PMSM with rotor saliency with the design consisting from the two steps. At first, two of the three nonlinearities in equations are compensated directly by adding an appropriate feedforward voltage signal. In the second step, nonlinear controller, which deals with the third nonlinearity, is designed by input-output linearization.

2. Nonlinear model of the PMSM with salient poles

The mathematical model of the PMSM in the d - q rotor reference frame involving saliencies is:

$$\frac{di_d}{dt} = -\frac{R}{L_d}i_d + \frac{pL_q}{L_d}\omega i_q + \frac{1}{L_d}u_d \quad (1)$$

$$\frac{di_q}{dt} = -\frac{R}{L_q}i_q - \frac{pL_d}{L_q}\omega i_d + \frac{1}{L_q}u_q - \frac{\Psi_{PM}P}{L_q}\omega \quad (2)$$

$$\frac{d\omega}{dt} = \frac{T_e}{J} - \frac{1}{J}T_L \quad (3)$$

$$T_e = \frac{3p}{2}(\Psi_{PM}i_q + (L_d - L_q)i_d i_q) \quad (4)$$

In (1)-(4) R , L_d , and L_q , are the per-phase armature resistance and the d -axis and q -axis inductances,

* E-mail address: karol.kyslan@tuke.sk

respectively; ψ_{PM} is the permanent-magnet flux, p is the number of pole pairs, J is the moment of inertia, T_e and T_L are the electromagnetic and the load torque, respectively; ω is rotor angular speed and i_d, i_q are the d -axis and q -axis component of the armature current, respectively. We consider the machine model as two input single output time invariant continuous system:

$$\begin{aligned} \dot{\bar{x}}(t) &= A(\bar{x}) + B\bar{u}(t) + Ez(t) \\ y &= C(\bar{x}) \end{aligned} \quad (5)$$

Choosing state variables: $x_1 = \omega, x_2 = i_q, x_3 = i_d, y = \omega, z = T_L, u_1 = u_q, u_2 = u_d$ we get nonlinear state-space representation of machine model (a_1 - a_7, b_{21}, b_{32}, e are corresponding constants) where the vector of the states and vector of the inputs are:

$$\bar{x} = [x_1 \ x_2 \ x_3]; \bar{u} = [u_1 \ u_2]; \quad (6)$$

the nonlinear state matrix:

$$A(\bar{x}) = \begin{bmatrix} a_1x_2 + a_2x_2x_3 \\ -a_3x_2 - a_4x_1x_3 - a_5x_1 \\ -a_6x_3 + a_7x_1x_2 \end{bmatrix} \quad (7)$$

the input and the error matrix:

$$B = \begin{bmatrix} 0 & 0 \\ b_{21} & 0 \\ 0 & b_{32} \end{bmatrix}; E = \begin{bmatrix} -e \\ 0 \end{bmatrix} \quad (8)$$

It should be noticed, that the first two rows of the state-space model represent the torque-speed subsystem and the last row represents the field current subsystem. Nonlinear controller in the state-space is designed in order to decouple both subsystems and to assure desired dynamics.

3. Direct compensation of nonlinearities in current equations

We introduce the compensations for nonlinearities that can be simply compensated by adding an opposite signals of nonlinearities to the corresponding control variables in this section. We define input variables for the system (5) as:

$$\begin{aligned} u_1 &= u_{10} + u_{com1} \\ u_2 &= u_{20} + u_{com2} \end{aligned} \quad (9)$$

where the inputs for the direct compensation of the nonlinearities are defined as:

$$\begin{aligned} u_{com1} &= \frac{1}{b_{21}} a_4 x_1 x_3; \\ u_{com2} &= -\frac{1}{b_{32}} a_7 x_1 x_2 \end{aligned} \quad (10)$$

and u_{10}, u_{20} are the new pre-defined control variables. Then simplified nonlinear state-space model is:

$$\begin{aligned} \begin{bmatrix} \dot{x}_1 \\ \dot{x}_2 \\ \dot{x}_3 \end{bmatrix} &= \begin{bmatrix} a_1x_2 + a_2x_2x_3 \\ -a_3x_2 - a_5x_1 \\ -a_6x_3 \end{bmatrix} + \\ &+ \begin{bmatrix} 0 & 0 \\ b_{21} & 0 \\ 0 & b_{32} \end{bmatrix} \begin{bmatrix} u_{10} \\ u_{20} \end{bmatrix} + \begin{bmatrix} -e \\ 0 \end{bmatrix} T_L \end{aligned} \quad (11)$$

Proposed compensations have brought significant simplification to the system because the two of the three nonlinearities are directly compensated. Now we design nonlinear controller for the system (11) with the use of nonlinear canonical form [15].

4. Design of the nonlinear controller

4.1 Controllability matrix

For the class of two-input nonlinear systems a controllability matrix is constructed as:

$$Q_R(\bar{x}) = \begin{bmatrix} \bar{b}_1(\bar{x}) N\bar{b}_1(\bar{x}) \dots N^{n_1-1}\bar{b}_1(\bar{x}) & \bar{b}_2(\bar{x}) N\bar{b}_2(\bar{x}) \\ \dots N^{n_2-1}\bar{b}_2(\bar{x}) \end{bmatrix} \quad (12)$$

where \bar{b}_1, \bar{b}_2 are the columns of the input matrix, n_1 and n_2 are the ranks of the subsystems, and $N\bar{b}(\bar{x})$ is defined for the constant input matrix B as:

$$N\bar{b}(\bar{x}) = \frac{\partial A(\bar{x})}{\partial \bar{x}} B(\bar{x}) \quad (13)$$

In our case $n_1=2$ and $n_2=1$, thus controllability matrix for the system (11) is:

$$Q_R(\bar{x}) = \begin{bmatrix} 0 & b_{21}(a_1 + a_2x_3) & 0 \\ b_{21} & -a_3b_{21} & 0 \\ 0 & 0 & b_{32} \end{bmatrix} \quad (14)$$

System is controllable until the controllability matrix is non-singular. It holds for the case of:

$$i_d \neq -\frac{\psi_{PM}}{L_d - L_q} \quad (15)$$

4.2 The transformation matrix

The transformation matrix for the nonlinear canonical form is [15]:

$$T(\bar{x}) = \begin{bmatrix} t_1(\bar{x}) \dots N^{n_1-1}t_1(\bar{x}) & t_2(\bar{x}) \dots N^{n_2-1}t_2(\bar{x}) \end{bmatrix}^T \quad (16)$$

where

$$Nt_i(\bar{x}) = \left[\frac{\partial t_i(\bar{x})}{\partial \bar{x}} \right]^T A(\bar{x}) \quad (17)$$

The rows of the transformation matrix are obtained by solving a set of partial differential equations:

$$\left[\frac{\partial t_i(\bar{x})}{\partial \bar{x}} \right]^T = k_i(\bar{x}) \bar{q}_{Ri}^T(\bar{x}); i = 1, 2, \dots \quad (18)$$

where $k_i(\bar{x})$ is a user-defined function and $\bar{q}_{Ri}^T(\bar{x})$ is the last row of each subsystem for inverse controllability matrix. In our case the last rows are defined as:

$$\bar{q}_{R1}^T = \left[\frac{1}{b_{21}(a_1 + a_2x_3)} \quad 0 \quad 0 \right]; \bar{q}_{R2}^T = \left[0 \quad 0 \quad \frac{1}{b_{32}} \right]$$

The user-defined functions have conveniently been chosen as:

$$k_1(\bar{x}) = b_{21}(a_1 + a_2x_3); k_2(\bar{x}) = b_{32}(a_1 + a_2x_3); \quad (19)$$

Thus the transformation matrix is:

$$T(\bar{x}) = \begin{bmatrix} x_1 \\ a_1x_2 + a_2x_2x_3 \\ x_3 \end{bmatrix} = \begin{bmatrix} x_{R1} \\ x_{R2} \\ x_{R3} \end{bmatrix} \quad (20)$$

4.3 Nonlinear canonical form

Nonlinear controllers have been designed by feedback linearization method according to [15]. With the transformation matrix (20) the transformation to the nonlinear controllability form is performed as following:

$$\dot{\bar{x}}_R = \left[\frac{\partial T(\bar{x})}{\partial \bar{x}} \right] [A(\bar{x}) + B(\bar{x})\bar{u}] \quad (21)$$

New state variables for transformed system are introduced, denoted as x_{Ri} . New transformed matrices are defined as:

$$A_R(\bar{x}) = \begin{bmatrix} a_1x_2 + a_2x_2x_3 \\ (a_1 + a_2x_3)(-a_3x_2 - a_5x_1) - a_2a_6x_2x_3 \\ -a_6x_3 \end{bmatrix} = \begin{bmatrix} x_{R2} \\ f_{R2}(\bar{x}) \\ f_{R3}(\bar{x}) \end{bmatrix} \quad (22)$$

$$B_R(\bar{x}) = \begin{bmatrix} 0 & 0 \\ b_{21}(a_1 + a_2x_3) & a_2x_2b_{32} \\ 0 & b_{32} \end{bmatrix} \quad (23)$$

The input matrix B_R can be decomposed as:

$$B_R(\bar{x}) = I_R M = \begin{bmatrix} 0 & 0 \\ 1 & 0 \\ 0 & 1 \end{bmatrix} \begin{bmatrix} b_{21}(a_1 + a_2x_3) & a_2x_2b_{32} \\ 0 & b_{32} \end{bmatrix} \quad (24)$$

If the input matrix is defined as follows:

$$\bar{u} = M^{-1}(\bar{x}) \begin{bmatrix} -f_{R2}(\bar{x}) + v_{R2} - r_2x_{R2} \\ -f_{R3}(\bar{x}) + v_{R3} - r_2x_{R3} \end{bmatrix} \quad (25)$$

and are further introduced to the system (21), both subsystems becomes autonomous and following system with a new inputs v_{R2} and v_{R3} is obtained:

$$\dot{\bar{x}}_R = \begin{bmatrix} 0 & 1 & 0 \\ 0 & -r_2 & 0 \\ 0 & 0 & -r_3 \end{bmatrix} \bar{x}_R + \begin{bmatrix} 0 & 0 \\ 1 & 0 \\ 0 & 1 \end{bmatrix} \begin{bmatrix} v_{R2} \\ v_{R3} \end{bmatrix} \quad (26)$$

It can be observed that the system (26) is linear. It is shown in Fig. 1 with the linear state-space controllers included. It is a “dummy” system, because neither the system nor its controllers will appear in the final control implementation. We introduce full state-space controllers with integral action in order to compensate the disturbances:

$$v_{Ri} = K_i \int (w_{Ri} - x_{Ri}) dt; i = 1, 2, 3 \quad (27)$$

It should be noted that using the integral part of controller according to (27) a new state variables $v_{R1}-v_{R3}$ occurs. Furthermore, the system in Fig. 1 presents the cascade control structure with the inner current loop and superimposed speed control loop. Torque-speed subsystem and field subsystem are independently controlled. Unknown parameters of the linear state-space controllers can be found by the well-known pole-placement method.

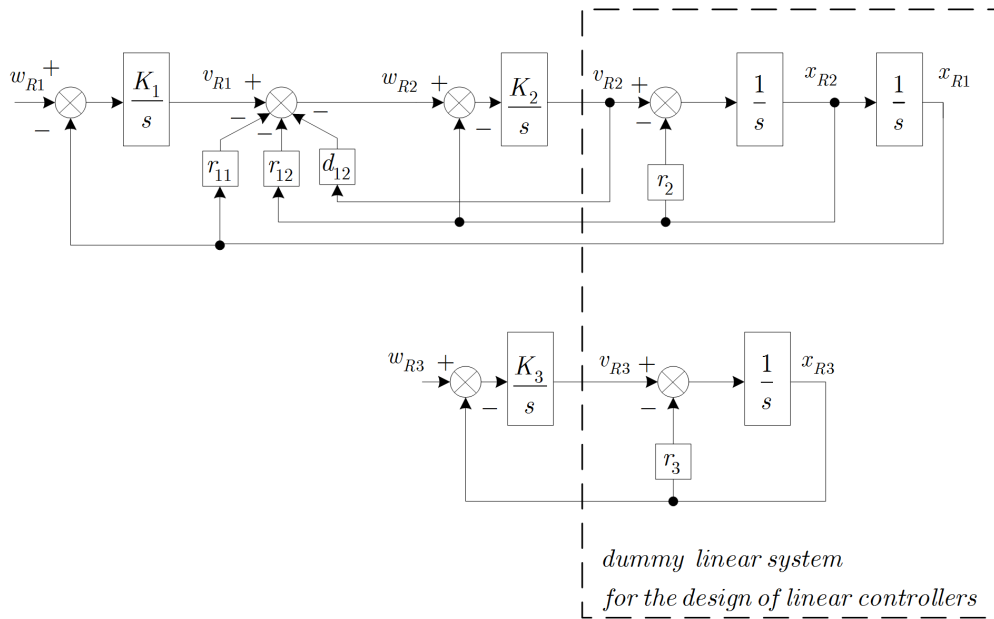


Fig. 1. Dummy linear system with the state-space controllers

5. Backward transformation

The vector of the control variables \bar{u} according to (25) defines the nonlinear control law. It is formulated in transformed state-space variables and so the backward transformation is needed. Substitution of the transformed variables (x_{Ri} , v_{Ri}) is based on the definition of the transformation matrix (20). The nonlinear control law after the substitution is:

$$u_{10} = \frac{1}{b_{21}} \left[v_2 - r_2 x_2 + a_3 x_2 + a_5 x_1 + \frac{a_2 x_2 (r_3 x_3 - v_3)}{a_1 + a_2 x_3} \right] \quad (28)$$

$$u_{20} = \frac{1}{b_{32}} (v_3 - r_3 x_3 + a_6 x_3) \quad (29)$$

Based on the transformation matrix, the reference variable is defined as:

$$w_2 = \frac{w_{R2}}{a_1 + a_2 x_3} \quad (30)$$

Then following holds:

$$w_2 = \frac{1}{a_1 + a_2 x_3} \left[(v_1 - r_{11} x_1 - a_1 (r_{12} x_2 + d_{12} v_2)) - \right] \quad (31)$$

The general control law with the all controllers is shown in Fig. 2.

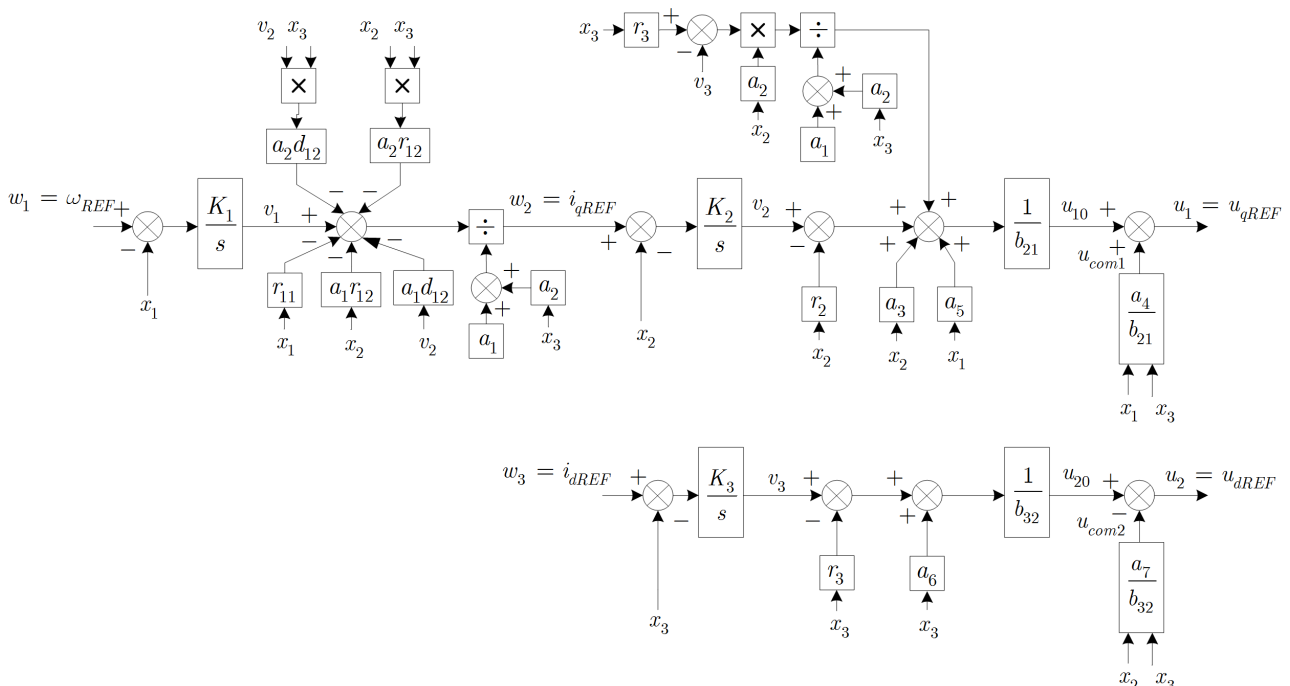


Fig. 2. Overall scheme with the nonlinear controller

6. Simulation Results

Designed control structure was simulated and compared with the classical field oriented vector control structure in dq -frame with the PI controllers. Responses are shown in Fig. 3 and Fig. 4, where the subscript ss indicates the responses of nonlinear controllers and subscript PI indicates the responses of the PI controllers. The parameters of PMSM have been obtained according to [16] and are summed in Tab.1. Both controllers were designed in the way to achieve the same rise time t_r . PI speed controller was designed according to the symmetrical optimum criterion, resulting in the $t_r = 8$ ms. The value of t_r with the damping coefficient $d = 0,6$ has been used as the performance index for the state-space controller, designed by the pole-placement method. The speed setpoint for the simulation was 70 rad/s. In $t = 0,02$ s current d -component was set to -1,6 A to weaken magnetic field of the rotor and in $t = 0,02$ s, the motor was loaded with the nominal load. There are small differences in the current responses because the current loop with PI controllers behaves as the first-order system in contrast to the nonlinear controller behaving as the second-order system. Parameters of the PI controller and nonlinear controller were recalculated according to changed saliency ratio for both Fig. 3 and Fig. 4. It can be seen that if the saliency ratio is increased, the nonlinear state-space controller keeps the same dynamic under the load conditions, whereas the dynamic of the PI controller is slightly deteriorated.

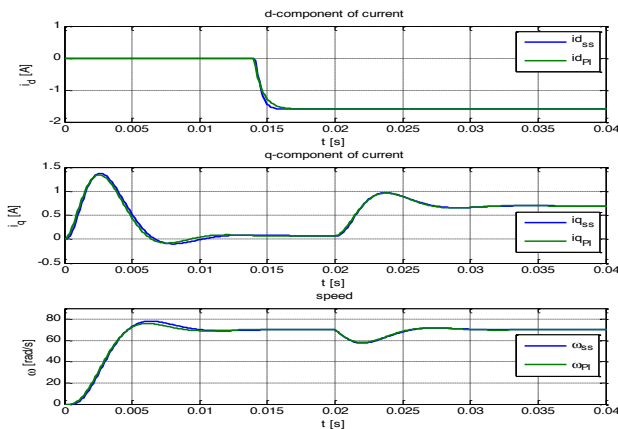


Fig. 3. Step responses, $L_d/L_q=2,18$

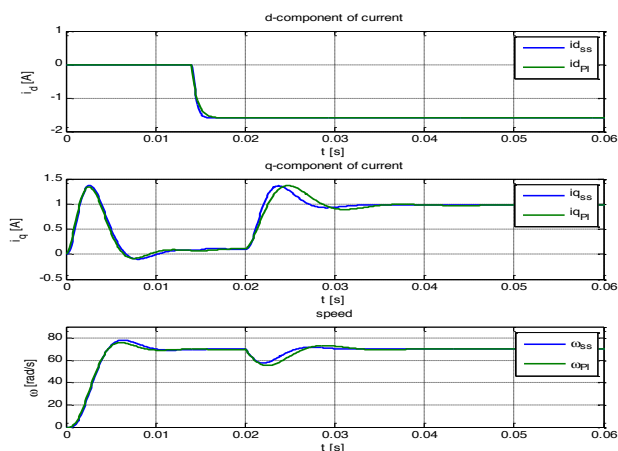


Fig. 4. Step responses, $L_d/L_q=6,18$

Table 1. Parameters of PMSM

P	mechanical power	200	W
n	nominal speed	3500	rpm
I_{max}	max. current	1,6	A
R	armature resistance	7	Ω
L_d	d-axis inductance	8,75	mH
L_q	q-axis inductance	4	mH
p	pole pair	5	
ψ_{PM}	flux of PM	0,104	Wb
J	total inertia	0,000043	kg/m ²

7. Conclusion

The input-output linearization of the PMSM model enables the analytical expression of the nonlinear controller with the acceptable number of the controller parameters, which can be even reduced by the singular perturbation method. The transformation to the appropriate coordinates has been found and the system becomes linear. Anyway, the same solution can be obtained by using the exact linearization with the application of the Lie's algebra, but it would require larger calculus. It is possible to find analytical solution of the nonlinear controller for the system even without feedforward, but resulted large number of the controller parameters would be unpractical to further implementation. Designed control structure compensates all nonlinearities in the mathematical model of the PMSM and comparing to traditional PI controllers, it shows similar performance. During field weakening, the nonlinearity affects the electromotive torque, but the performance of the nonlinear controller is preserved. With the increasing saliency ratio, the nonlinear controller shows better performance than the PI controller.

The contribution of this paper lies in the detailed description of the nonlinear controller design, which is based on the nonlinear canonical form. The dynamics of proposed nonlinear controller is fully adjustable, comparing to the PI controller, where only two parameters can be tuned. In addition, the dynamics of the proposed controller is preserved in the all operating points and regardless of the saliency ratio.

However, the complexity of the proposed control scheme, which in spite of everything contains a lot of parameters, brings only the slight improvement of the performance and only in specific cases, as was shown in the simulations. In the practical usage, where the system parameters may vary, an expected improvement of the presented control scheme would be negligible and less reliable than using well-established PI controllers.

Acknowledgement

This work was supported by the Scientific Grant Agency of the Ministry of Education of the Slovak Republic and Slovak Academy of Sciences (VEGA), under the project code 1/0464/15.

References

- Genduso, F.; Miceli, R.; Rando, C.; Galluzzo, G.R.; , "Back EMF Sensorless-Control Algorithm for High-Dynamic Performance PMSM," *IEEE Transactions on Industrial Electronics*, vol.57, no.6, pp.2092-2100, June 2010.
- Peroutka, Z.; Smidl, V.; Vosmik, D.; "Challenges and limits of extended Kalman Filter based sensorless control of permanent magnet synchronous machine drives," *13th European Conference on Power Electronics and Applications, 2009. EPE '09*, vol., no., pp.1-11, 8-10 Sept. 2009.
- Hongryel Kim; Jubum Son; JangMyung Lee; , "A High-Speed Sliding-Mode Observer for the Sensorless Speed Control of a PMSM," *Industrial Electronics, IEEE Transactions on* , vol.58, no.9, pp.4069-4077, Sept. 2011
- Hammel, W.; Kennel, R.M.;, "Position sensorless control of PMSM by synchronous injection and demodulation of alternating carrier voltage," *Sensorless Control for Electrical Drives (SLED), 2010 First Symposium on* , vol., no., pp.56-63, 9-10 July 2010.
- Raca, D.; Garcia, P.; Reigosa, D.D.; Briz, F.; Lorenz, R.D., "Carrier-Signal Selection for Sensorless Control of PM Synchronous Machines at Zero and Very Low Speeds," *IEEE Transactions on Industry Applications*, vol.46, no.1, pp.167,178, Jan.-feb. 2010.
- Xiaoguang Zhang; Lizhi Sun; Ke Zhao; Li Sun, "Nonlinear Speed Control for PMSM System Using Sliding-Mode Control and Disturbance Compensation Techniques," *IEEE Transactions on Power Electronics*, vol.28, no.3, pp.1358-1365, March 2013.
- Diblik, M.; Cernohorsky, J., "Advanced servo-drive reference-model control application," *13th International Carpathian Control Conference (ICCC), 2012*, pp.109-114, 28-31 May 2012 doi: 10.1109/CarpathianCC.2012.6228625.
- Jezernik, Karel; Rodic, Miran; Horvat, Robert; , "FPGA based control strategy for the reduction of torque ripple for PMSM," *15th International Power Electronics and Motion Control Conference (EPE/PEMC), 2012*, vol., no., pp.LS6a.1-1-LS6a.1-8, 4-6 Sept. 2012
- Sam-Young Kim; Chinchul Choi; Kyeongjin Lee; Wootaik Lee; , "An Improved Rotor Position Estimation With Vector-Tracking Observer in PMSM Drives With Low-Resolution Hall-Effect Sensors," *IEEE Transactions on Industrial Electronics* , vol.58, no.9, pp.4078-4086, Sept. 2011.
- Errouissi, R.; Ouhrouche, M.; Wen-Hua Chen; Trzynadlowski, A.M.; "Robust Nonlinear Predictive Controller for Permanent-Magnet Synchronous Motors with an Optimized Cost Function," *IEEE Transactions on Industrial Electronics*, vol.59, no.7, pp.2849-2858, July 2012.
- Vittek, J; Ftorek, B; "Energy efficient speed and position control of electric drives with PMSM", *Komunikacie*, vol. 16, no. 1, pp. 64-71, February 2014.
- Yi Wang; Jianguo Zhu; Youguang Guo; "A Comprehensive Analytical Mathematic Model for Permanent-Magnet Synchronous Machines Incorporating Structural and Saturation Saliencies," *IEEE Transactions on Magnetics*, vol.46, no.12, pp.4081-4091, Dec. 2010.
- Zboray, L; Ďurovský, F; „State-Space Control of Electrical Drives“, *Vienala* 1995. ISBN 80-967 249-1-6. (In Slovak).
- Viet Quoc Leu; Han Ho Choi; Jin-Woo Jung, "Fuzzy Sliding Mode Speed Controller for PM Synchronous Motors With a Load Torque Observer," *IEEE Transactions on Power Electronics*, vol.27, no.3, pp.1530,1539, March 2012.
- Sommer, R; „Entwurf zeitvarianter Systeme durch Polvograbe“, *Regelungstechnik*, 1978. pp. 189-196.
- Šlapak, V.; Kyslan, K.; Mejdr, F.; Durovsky, F.; Determination of Initial Commutation Angle Offset of Permanent Magnet Synchronous Machine - An Overview and Simulation, In: *Acta Electrotechnica et Informatica*, vol. 14, no. 4, 2014, pp. 17-22, doi: 10.15546/aeii-2014-0035